Investigating the Dissolution Behavior of Calcium Carbonate Bio-Cemented Sands

Bruna G. O. Ribeiro¹ and Michael G. Gomez, Ph.D., A.M.ASCE²

¹Ph.D. Student, Dept. of Civil and Environmental Engineering, Univ. of Washington, Seattle, WA. Email: brunagr@uw.edu

²Assistant Professor, Dept. of Civil and Environmental Engineering, Univ. of Washington, Seattle, WA. Email: mggomez@uw.edu

ABSTRACT

Microbially Induced Calcite Precipitation (MICP) is a bio-mediated cementation process that uses microbial enzymatic activity to catalyze the precipitation of CaCO₃ minerals on soil particle surfaces and contacts. Extensive research has focused on understanding various aspects of MICP-treated soils including soil behavioral enhancements and process reaction chemistry, however, almost no research has explored the permanence of bio-cemented geomaterials. As the technology matures, an improved understanding of the longevity of bio-cementation improved soils will be critical towards identifying favorable field applications, quantifying environmental impacts, and understanding their long-term performance. In this study, a series of batch experiments were performed to investigate the dissolution kinetics of CaCO₃-based biocemented sands with the specific aim of incorporating these behaviors into geochemical models. All batch experiments involved previously bio-cemented poorly graded sands that were exposed to different dissolution treatments intended to explore the magnitude and rate of CaCO₃ dissolution as a function of acid type, concentration, initial pH, and other factors. During experiments, changes in solution pH and calcium concentrations indicative of CaCO₃ dissolution were monitored. After experiments, aqueous measurements were compared to those simulated using two different dissolution kinetic frameworks. While not exhaustive, the results of these experiments suggest that the dissolution behavior of bio-cementation can be well-approximated using existing chemically controlled kinetic models, particularly when surrounding solutions are more strongly buffered.

INTRODUCTION

Microbially Induced Calcite Precipitation (MICP) is a promising bio-mediated cementation process that can improve the geotechnical properties of soils through the precipitation of calcium carbonate (CaCO₃) on soil particle surfaces and contacts (Stocks-Fisher et al. 1999; Martinez and DeJong 2009; and others). Bio-cementation can increase the initial shear stiffness, peak shear strength, and liquefaction resistance of soils, while decreasing soil porosity and hydraulic conductivity (Montoya and DeJong 2015; Minto et al. 2016; Gomez and DeJong 2017). Despite many recent advances in the technology, almost no research to date has explored the life cycle performance of bio-cementation and investigated material permanence. Limited understanding of the processes by which bio-cemented soils can chemically degrade has restricted our ability to evaluate the long-term resilience of MICP and quantify process impacts. Once applied at field-scale, bio-cementation mineralogy, dissolution kinetics, and subsurface geochemical conditions will play an important role, governing the rate of bio-cementation degradation. Recent studies have shown that important changes in bio-cementation mineralogy can result from both changes

in environmental conditions and treatment techniques (Burdalski and Gomez 2020). Although the dissolution behavior of CaCO₃-based bio-cementation has yet to be explored, a wealth of past studies have examined the dissolution behavior of both naturally-occurring and abioticallygenerated CaCO₃ minerals (Sjöberg 1978; Morse 2002; Cubillas et al. 2005; Gehlen et al. 2005; Colombani 2016; and others). In these studies, some significant discrepancies in dissolution behaviors have been observed with two different dissolution kinetic models being primarily used to describe the dissolution behavior of CaCO₃ minerals. The ability of these models to accurately capture dissolution behaviors have been found to largely depend on both the initial pH and temperature of surrounding solutions (Sjöberg and Rickard 1984). Collectively, these studies have suggested that when the pH of surrounding solutions exceeds 5.5, the rate of CaCO₃ dissolution may be primarily chemically-controlled with dissolution rates proportional to the surrounding solution's saturation index. Eq. 1 presents the chemically-controlled dissolution kinetic equation, where r_c is the dissolution rate, k_c is a dissolution rate constant, A_c is the mineral specific surface area, n is the reaction order, K_{sp} is the solubility product of the mineral, and (Ca²⁺) and (CO₃²⁻) are the activities of calcium and carbonate ions, respectively (Morse and Berner 1972). In contrast, under increasingly acidic conditions (corresponding to pH values below 4), CaCO₃ dissolution rates have been shown to be increasingly diffusion-controlled with dissolution rates primarily dependent on the pH of surrounding solutions. Eq. 2 presents the diffusion-controlled kinetic equation, where r_c is the dissolution rate, k_c is a dissolution rate constant, A_c is the mineral specific surface area, (H⁺) is the activity of hydrogen ions, and n is the reaction order (Sjöberg and Rickard 1984). While both kinetic models have been used to effectively predict the dissolution behavior of CaCO₃ minerals under varying solution conditions, it remains unclear if similar frameworks can be used to capture the dissolution behavior of biocementation.

$$r_c = k_c A_c \left(1 - \frac{(ca^{2+})(co_3^{2-})}{\kappa_{sp}} \right)^n \tag{1}$$

$$r_c = k_c A_c (H^+)^n \tag{2}$$

In this study, a series of batch experiments were performed to investigate the dissolution behavior of CaCO₃-based bio-cemented sands with the specific aim of calibrating existing geochemical modeling approaches to capture changes in aqueous chemistry during the dissolution process. Although assessment of bio-cementation permeance may be site-specific, such geochemical models may afford the opportunity to forward-predict changes in biocementation magnitudes and distributions for assessment of improvement longevity under site specific conditions. Batch experiments employed in this study included previously bio-cemented poorly-graded sand specimens that were subjected to different dissolution treatments intended to explore the magnitude and rate of CaCO₃ dissolution as a function of acid type, concentration, initial pH, and other factors. During experiments, changes in solution pH and aqueous calcium concentrations indicative of CaCO₃ dissolution were monitored in time to track dissolution rates. Following all experiments, two dissolution kinetic frameworks were incorporated into the geochemical code PHREEQC (Parkhurst and Appelo 2013) and were used to model similar aqueous trends. In both dissolution kinetic frameworks, unknown kinetic parameters including the reaction order (n), dissolution rate constant (k_c), and the mineral specific surface area (A_c), were adjusted to capture experimental trends. The ability of these frameworks to capture observed dissolution behaviors as well as changes in bio-cementation dissolution with variations in aqueous chemical conditions are discussed.

MATERIALS AND METHODS

Dissolution Batch Experiments

Dissolution batch experiments were performed in sealed glass bottles and included 20 grams of dried bio-cemented sand samples mixed with 100 mL of dissolution solutions. Seven different dissolution solutions were considered and included dilute hydrochloric acid (HCl) and acetic acid solutions with varying sodium acetate and sodium chloride (NaCl) additions. The considered dissolution solutions were intended to (1) allow for the investigation of the effect of variations in acid type, concentration, and buffering capacity and the ability of existing dissolution kinetic models to capture these dissolution behaviors and (2) permit CaCO₃ dissolution magnitudes sufficient to reliably capture changes in solution aqueous calcium concentrations and pH indicative of biocementation dissolution over experimentally practical time scales. Although these solutions were not intended to represent site-specific geochemical conditions nor extreme chemical events, the selected solutions were intended to allow for dissolution behaviors to be better fundamentally understood. Table 1 summarizes the composition of all dissolution solutions including their chemical concentrations and initial pH values.

Table 1. Summary of Dissolution Solution Chemical Compositions

Dissolution Solution	No. of Experiments	HCI (mM)	Acetic Acid (mM)	Sodium Acetate (mM)	Sodium Chloride (mM)	Initial pH
10H	3	10	-	-	-	2.21
10A	3	-	10	-	-	3.51
10A_50Act	1	-	10	50	-	5.38
10A_100Act	1	-	10	100	-	5.61
10A_100NaCl	1	-	10	-	100	3.31
50A	1	-	50	-	-	3.20
50A_100Act	1	-	50	100	-	4.85

Bio-cemented sand samples used in batch experiments were obtained from previous soil column experiments (Lee et al. 2019) involving a poorly-graded Concrete Sand material ($D_{50} \approx 1.07\,$ mm, fines $\approx 1.1\%$) wherein the bio-cementation process was mediated by indigenous ureolytic microorganisms. Bio-cemented sand samples had CaCO3 contents near 5.0% by mass, as determined by pressure chamber measurements (ASTM 2014) and supplied dry soil masses were intended to provide excess CaCO3 to ensure that the dissolution process could proceed to equilibrium. After mixing dry sand samples with dissolution solutions, glass bottles were sealed and continuously mixed using a double-orbital shaker at a shaking speed of 150 rpm for 48 hours to homogenize solutions. Aqueous samples were collected and pH measurements were obtained 30, 60, 120, 240, 360, 480, 600, 1200, 1800, 5400 and 172800 seconds after initially mixing. Samples collected for aqueous calcium measurements were 500 μ L in volume and were filtered after collection using 0.45 μ m centrifuge spin filters to remove all solid precipitates. The total sampled volume in each experiment never exceeded 10% of the total volume. All samples were immediately frozen after filtering until thawing for subsequent aqueous measurements.

Aqueous Chemical Measurements

Aqueous calcium measurements were completed using a QuantiChrom calcium assay kit (BioAssay Systems). Frozen samples were thawed, diluted to obtain calcium concentrations within the linear range of the assay (< 5.0 mM), mixed with a colorimetric reagent, and allowed to react for 10 minutes. Sample absorbances were measured using a microplate spectrophotometer at a wavelength of 612 nm. Sample pH measurements were completed immediately after collection using a semi-micro pH electrode and meter system that was calibrated daily using three buffers (4.01, 7.00, 10.00) and had ± 0.05 pH unit accuracy.

Table 2. Summary of Dissolution Kinetic Parameters for Chemically-controlled Models

Dissolution Solution	kcAc (s ⁻¹)	n
10H	6 x 10 ⁻⁵	14
10A	6 x 10 ⁻⁵	14
10A_50Act	6 x 10 ⁻⁵	14
10A_100Act	1 x 10 ⁻⁴	14
10A_100NaCl	6 x 10⁻⁵	14
50A	2 x 10 ⁻⁴	14
50A_100Act	2 x 10 ⁻⁴	14

Geochemical Modeling

The USGS geochemical code PHREEQC (Parkhurst and Appelo 2013) was used to model solution pH and aqueous calcium concentration changes in time for all dissolution experiments. Although equilibrium reactions related to carbonate species were already included in the PHREEQC speciation database (phreeqc.dat), equilibrium reactions related to sodium acetate were added from the llnl.dat database. Since equilibrium reactions related to acetic acid were not included in either database, these additional speciation reactions were added as user-defined reactions. In dissolution simulations, both the chemically-controlled (Eq. 1) and the diffusioncontrolled (Eq. 2) kinetic models were explored, and unknown kinetic parameters were varied to match experimentally observed trends. Given that both k_c and A_c were unknown, the product "k_cA_c" was treated as a single fitting parameter in all models. For initial simulations, the value of k_cA_c was assumed to be 3.24 x 10⁻⁷ s⁻¹ and the reaction order (n) was set to 1.25 following values presented in Cubillas et al. (2005) for calcite minerals. Variations in both k_cA_c and n were considered using sensitivities analyses performed following all experiments in order to better determine these unknown parameters and allow for an improved fit between the kinetic models and the experimental data. After performing the 10 mM HCl experiments, the reaction order was found to deviate significantly from earlier values from Cubillas et al. (2005) and reaction order values were instead set equal to 14 for all chemically-controlled models but maintained at 1.25 for all diffusion-controlled kinetic models. While some uncertainty exists in the exact value of the reaction order, the considered models were found to be largely insensitive to small variations in this value. Therefore, similar reaction order values were maintained for all chemicallycontrolled (n=14) and diffusion-controlled (n=1.25) models and subsequent sensitivity analyses considered only variations in the k_cA_c parameter. Table 2 presents all calibrated parameter values for chemically-controlled models along with their corresponding dissolution experiments. For all chemically-controlled models, k_cA_c varied between 6 x 10⁻⁵ s⁻¹ and 2 x 10⁻⁴ s⁻¹, with larger k_cA_c values observed for more strongly buffered solutions. In the chemically-controlled kinetic equation (Eq. 1), the solubility product (K_{sp}) of CaCO₃-based bio-cementation was assumed to be 10^{-8.48} following values for calcite (Stumm and Morgan 2012) and recent studies which confirmed the predominance of calcite minerals in bio-cemented sands under most reaction conditions (Gomez et al. 2019; Burdalski and Gomez 2020).

RESULTS AND DISCUSSION

Figure 1 presents aqueous calcium and pH trends in time for all 10 mM HCl experiments along with trends from both chemically-controlled ($k_cA_c = 6 \times 10^{-5}$, n = 14) and diffusioncontrolled dissolution kinetic models ($k_cA_c = 5 \times 10^{-1}$, n = 1.25). As shown, initial concentrations of calcium were near 0 mM and initial solution pH values were near 2.2. As CaCO₃ dissolution proceeded, calcium concentrations increased to near 3 mM after ≈100 seconds with pH values remaining nearly constant. A sharp increase in pH values was observed in all experiments near 700 seconds from values between 2.2 and 2.6 to near 6.8. After 5400 seconds (1.5 hours), both aqueous calcium concentrations and pH values appeared to stabilize indicating the end of CaCO₃ dissolution. 48 hour measurements indicated that final pH values were near 7.2 and final calcium concentrations were near 5.2 mM. When comparing both kinetic models to the experimental data, several interesting behaviors can be observed. While the diffusion-controlled model exhibited good agreement with the experiments up to ≈500 seconds, at greater times the model underpredicted the observed dissolution rate and final aqueous calcium concentrations. In contrast, the chemically-controlled model, agreed well with the experimental data after ≈700 seconds including final calcium concentrations, despite having relatively poor agreement at the beginning of reactions. Similar to other past studies on CaCO₃ dissolution, these results suggested that bio-cementation dissolution may have occurred in two different phases with a diffusion-controlled dissolution rate initially at low pH values and an increasingly chemicallycontrolled dissolution rate once pH values increased (after ≈700 seconds). While both models had somewhat limited agreement with both pH and calcium concentrations in time, the chemically-controlled kinetic appeared to well-approximate both final calcium concentrations and final pH values.

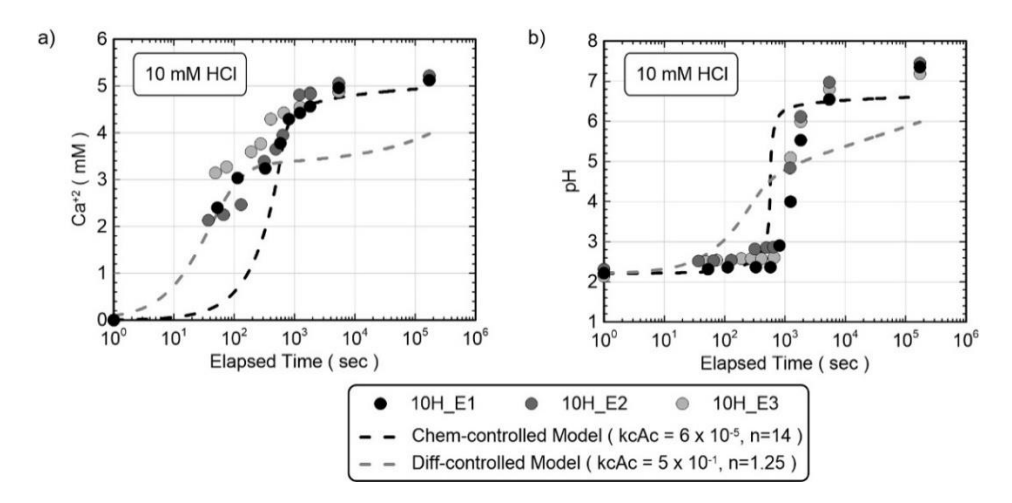


Figure 1. Experimental and modeled results for 10 mM HCl batch experiments including (a) calcium concentrations (mM) and (b) pH values in time.

Figure 2 presents aqueous calcium and pH trends in time from all 10 mM acetic acid experiments along with trends from both chemically-controlled ($k_cA_c = 6 \times 10^{-5}$ and n = 14) and diffusion-controlled dissolution kinetic models ($k_cA_c = 4 \times 10^1$ and n = 1.25). Acetic acid was selected for testing as it is a relatively weak organic acid (pKa= 4.35) in comparison to the much stronger HCl examined previously (pKa= -8). As shown, a rapid increase in calcium concentrations was again observed during the first ≈1200 seconds of the experiment indicative of CaCO₃ dissolution. During this same time period, solution pH progressively increased from values near 3.5 to 6.2 with a much more gradual rise when compared to the sharp increase observed in HCl experiments. After 48 hours, final calcium concentrations were near 6.8 mM and final pH values approached 7.1 in all experiments. Similar to the previous HCl experiments, changes in dissolution rates were again observed in time with the diffusion-controlled model better capturing initial trends when pH values were less than ≈5, and the chemically-controlled model better capturing later trends when pH values exceeded ≈5. Despite the diffusioncontrolled model exhibiting poor prediction of behaviors at later time, both models provided good estimates of final calcium concentrations. When examining pH trends, model predictions were again best for the diffusion-controlled model initially and the chemically-controlled model near the end of reactions, with both models well approximating final pH values.

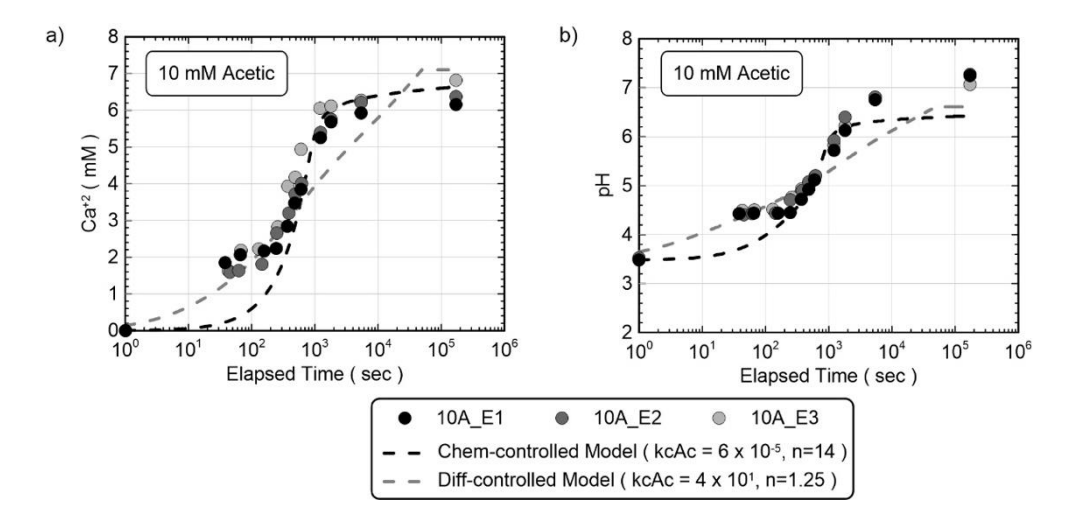


Figure 2. Experimental and modeled results for 10 mM acetic acid batch experiments including (a) Ca²⁺ concentrations and (b) pH values in time.

Figure 3 presents aqueous calcium and pH trends in time from experiments with 10 mM acetic acid (10A_E1), 10 mM acetic acid and 50 mM sodium acetate (10A_50Act); 10 mM acetic acid and 100 mM sodium acetate (10A_100Act), and 10 mM acetic acid and 100 mM sodium chloride (10A_100NaCl) along with calibrated chemically-controlled dissolution models for each experiment (parameters summarized in Table 2). Variations in acetic acid concentrations and supplied sodium acetate and sodium chloride concentrations were intended to examine the effects of acid concentrations, solution buffering capacities, and solution ionic strengths on dissolution behaviors. As shown, a spectrum of initial pH values and dissolution rates were observed with changes in supplied acetate concentrations. Initial pH values increased from ≈3.3 to ≈5.6 when supplied acetate concentrations increased from 0 to 100 mM. When supplied acetate was absent (10A_E1), the chemically-controlled model appeared to deviate

significantly from the experimental data initially during reactions when the pH was less than ≈5.0. However, when solutions became both more strongly buffered and initial pH values increased due to acetate additions (i.e., 10A_50Act, 10A_100Act), agreements between the modeled trends and the experimental data improved significantly initially during experiments with both final pH and calcium values well captured. While it was hypothesized that agreements between the chemically-controlled modeled trends and experimental data improved due to increases in initial solution pH with supplied acetate, it also remained possible that increases in solution buffering, which minimized pH changes early on during reactions may have also contributed towards improving the ability of these models to capture the experimental trends. When solution ionic strengths increased due to the addition of 100 mM sodium chloride (10A_100NaCl), no substantial differences were observed when comparing this experiment to the acetic acid only experiment (10A_E1). This suggested that while changes in solution buffering and initial pH values may dramatically alter bio-cementation dissolution behaviors in time, ionic strength changes likely only had minimal impacts on the observed trends.

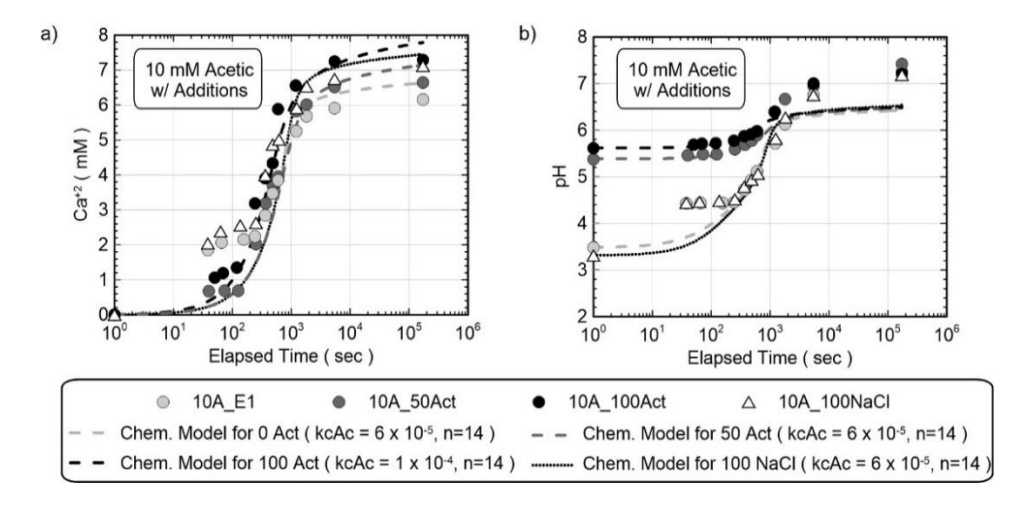


Figure 3. Experimental and modeled results for 10 mM acetic acid batch experiments with acetate and NaCl additions including (a) Ca²⁺ concentrations and (b) pH values versus time.

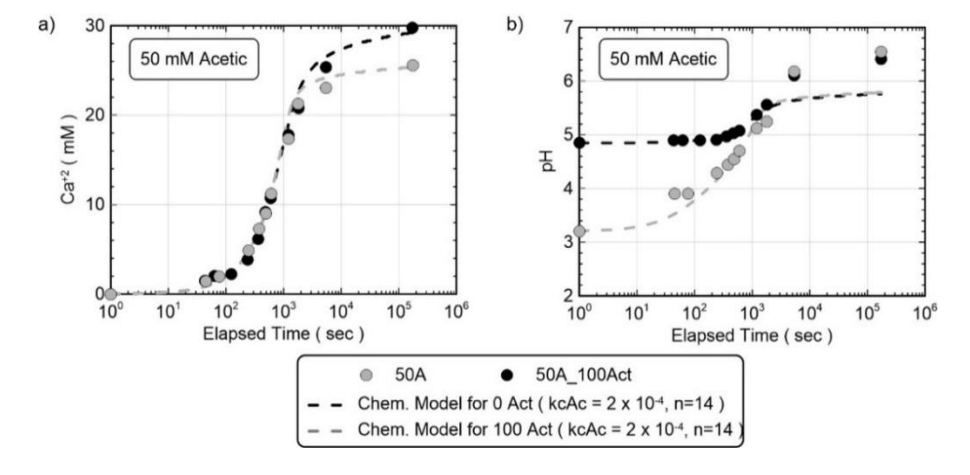


Figure 4. Experimental and modeled results for 50 mM acetic acid batch experiments including (a) Ca²⁺ concentrations and (b) pH values versus time.

Figure 4 presents aqueous calcium and pH trends in time from experiments with 50 mM acetic acid (50A) and 50 mM acetic acid with 100 mM acetate (50A_100Act) along with calibrated chemically-controlled models (parameters summarized in Table 2). As shown, calcium trends from both experiments and models were quite similar during the first 1800 seconds (30 minutes), with more significant deviations observed near the end of reactions. When comparing pH trends, pH values differed significantly between experiments during the first 1200 seconds (20 minutes) with higher pH values near 5.0 observed in the more strongly buffered experiment (50A_100Act) and lower pH values between 3.0 and 4.0 observed in the 50 mM acetic acid only experiment (50A). At later time in both experiments, final pH values converged near 6.4. Although it was hypothesized that the chemically-controlled model would poorly capture the initial dissolution behavior of the 50 mM acetic acid experiment (50A) due to its low initial pH (≈3.2), interestingly the model appeared to well approximate both pH and calcium concentrations trends in time. This suggested that although dissolution rates may be strongly influenced by the initial pH of surrounding solutions, the buffering capacity of such solutions may also be an important factor governing the dissolution behavior of bio-cementation.

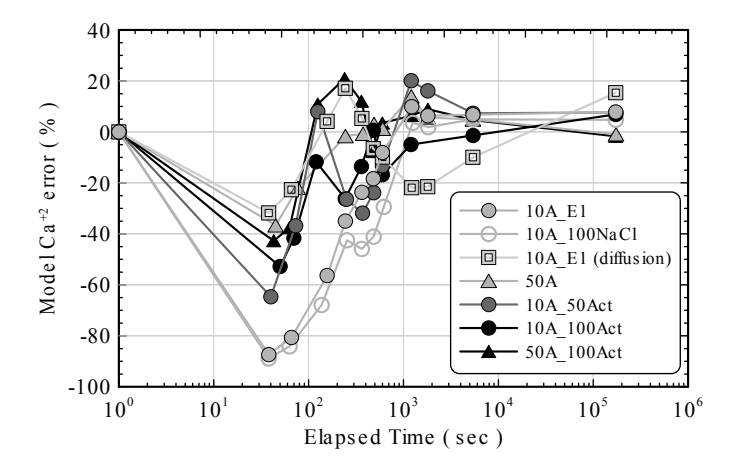


Figure 5. Comparison of model Ca²⁺ errors for all acetic acid experiments. All errors are for chemically-controlled models with the exception of the 10A_E1 diffusion-controlled model.

While the results of the 50 mM acetic acid experiments were encouraging, it should be mentioned that by changing both acid and buffer concentrations, the magnitudes of CaCO₃ dissolution exhibited in each experiment also varied significantly. For example, while final calcium concentrations were between 5 and 7 mM in the 10 mM HCl and acetic acid experiments, final calcium concentrations were much larger and between 25 and 30 mM in 50 mM acetic acid experiments. In order to more equally compare the ability of these models to capture dissolution trends in time, model calcium errors were calculated as the difference between the modeled and measured calcium concentrations normalized by measured calcium concentrations (Eq. 3). Figure 5 presents a comparison of model calcium errors for all acetic acid experiments and corresponding chemically-controlled kinetic models in time. For the 10 mM acetic acid experiment (10A_E1) specifically, model errors from the diffusion-controlled kinetic model are also provided. As shown, all models underpredicted calcium concentrations initially during experiments, with errors between ≈30% and 90% near 50 seconds of reaction time. As

expected, errors were largest for 10 mM acetic acid experiments which contained no added acetate, with improvements in model estimates with either increases in acetic acid concentrations or greater supplied acetate concentrations. It should be mentioned that significant model discrepancies at early time may also reflect experimental measurement errors due to rapidly changing chemical conditions. At times near 1000 seconds (15 minutes), errors for all chemically-controlled models appeared to converge to between 5% underprediction and 20% overprediction. After 1.5 hours, all chemically-controlled model errors were generally less than ≈10%. Although for the 10 mM acetic acid experiment, the diffusion-controlled model yielded improved estimates over the first 500 seconds, again at larger times errors were substantially greater with a significant overprediction of the final calcium concentration. Although estimates from diffusion-controlled models are not presented for more strongly buffered experiments, in all simulations considered the ability of such models to capture trends near equilibrium was inferior to similar chemically-controlled models.

$$Model\ Ca^{+2}Error\ (\%) = \frac{Ca_{modeled}^{+2} - Ca_{measured}^{+2}}{Ca_{measured}^{+2}}$$
(3)

CONCLUSIONS

In this study, a series of batch experiments were performed to investigate the dissolution behavior of CaCO₃-based bio-cemented sands as a function of acid concentration, acid type, initial pH, solution buffering capacity, and solution ionic strength. Following these experiments, the ability of existing dissolution kinetic models to capture temporal changes in aqueous calcium concentrations and solution pH was assessed. In batch experiments, changes in CaCO3 dissolution rates and magnitudes were observed with changes in the chemical composition of surrounding solutions. For solutions with dilute acid concentrations (e.g., 10 mM acetic acid and HCl), changes in dissolution behaviors were observed in time with a diffusion-controlled model better approximating behaviors initially and a chemically-controlled model better capturing trends near equilibrium. For experiments involving 10 mM acetic acid with varying sodium acetate concentrations, chemically-controlled kinetic models were able to well approximate calcium and pH trends for all experiments suggesting that such models may perform better when either initial pH values are higher and/or solutions are more strongly buffered. When experiments were performed with more concentrated acetic acid solutions, experimental trends were well approximated by the chemically-controlled model regardless of sodium acetate additions and despite low initial pH values near 3.2. Collectively, these results suggest that the buffering capacity of surrounding solutions may be an important factor influencing the dissolution behavior of bio-cementation with more strongly buffered solutions behaving more similar to trends estimated using a chemically-controlled kinetic. When comparing modeled calcium errors between experiments, similar trends were observed with most models estimating calcium concentrations to within ≈20% of experimental values after ≈2 minutes of reaction time. While not exhaustive, the obtained results suggest that the dissolution behavior of CaCO₃-based bio-cementation can be reasonably captured using existing kinetic models for applications including the prediction of bio-cementation permanence. It should be mentioned, however, that geochemical models presented in this study were calibrated to capture chemical changes during the entire monitoring period. If such models are to be employed for the prediction of biocementation spatial dissolution patterns, kinetic parameters will likely need to be calibrated to capture dissolution behaviors over time scales relevant to the specific reactive transport conditions present. Future work is also needed to further understand the ability of these models to capture bio-cementation dissolution spatial and temporal changes under reactive transport conditions more representative of in-situ soils.

ACKNOWLEDGEMENTS

Funding for this research work was provided by the National Science Foundation (ECI-1824647) and is greatly appreciated. Research collaboration made possible through the National Science Foundation under NSF Cooperative Agreement No. EEC-1449501 is also greatly appreciated. Any opinions, findings, and conclusions or recommendations expressed in this manuscript are those of the authors and do not necessarily reflect the views of the National Science Foundation.

REFERENCES

- ASTM. (2014). Standard test method for rapid determination of carbonate content of soils. ASTM D4373-14, West Conshohocken, PA.
- Burdalski, R., and Gomez, M. G. (2020). "Investigating the Effects of Biogeochemical Conditions During Microbially Induced Calcite Precipitation (MICP) Soil Improvement", *Geo-Congress 2020: Biogeotechnics*, ASCE, Reston, VA.
- Colombani, J. (2016). "The alkaline dissolution rate of calcite." *The Journal of Physical Chemistry Letters*, 7(13), 2376-2380.
- Cubillas, P., Köhler, S., Prieto, M., Chaïrat, C., and Oelkers, E. H. (2005). "Experimental determination of the dissolution rates of calcite, aragonite, and bivalves." *Chemical Geology*, 216(1-2), 59-77.
- Gehlen, M., Bassinot, F. C., Chou, L., and McCorkle, D. (2005). "Reassessing the dissolution of marine carbonates: II. Reaction kinetics." *Deep Sea Research Part I: Oceanographic Research Papers*, 52(8), 1461-1476.
- Gomez, M. G., and DeJong, J. T. (2017). "Engineering properties of bio-cementation improved sandy soils." *Grouting 2017*, 23-33. ASCE, Reston, VA.
- Gomez, M. G., Graddy, C. M., DeJong, J. T., and Nelson, D. C. (2019). "Biogeochemical changes during bio-cementation mediated by stimulated and augmented ureolytic microorganisms." *Scientific Reports*, 9(1), 1-15.
- Lee, M., Kolbus, C. M., Yepez, A. D., and Gomez, M. G. (2019). "Investigating Ammonium By-Product Removal following Stimulated Ureolytic Microbially-Induced Calcite Precipitation." *Geo-Congress 2019: Soil Improvement*, ASCE, Reston, VA, 260-272.
- Martinez, B. C., and DeJong, J. T. (2009). "Bio-mediated soil improvement: load transfer mechanisms at the micro-and macro-scales." *Advances in ground improvement: research to practice in the United States and China*, ASCE, Reston, VA. 242-251.
- Minto, J. M., MacLachlan, E., El Mountassir, G., and Lunn, R. J. (2016). "Rock fracture grouting with microbially induced carbonate precipitation." *Water Resources Research*, 52(11), 8827-8844.
- Montoya, B. M., and DeJong, J. T. (2015). "Stress-strain behavior of sands cemented by microbially induced calcite precipitation." *Journal of Geotechnical and Geoenvironmental Engineering*, 141(6), 04015019.

- Morse, J. W., and Berner, R. A. (1972). "Dissolution kinetics of calcium carbonate in sea water; I, A kinetic origin for the lysocline." *American Journal of Science*, 272(9), 840-851.
- Morse, J. W., and Arvidson, R. S. (2002). "The dissolution kinetics of major sedimentary carbonate minerals." *Earth-Science Reviews*, 58(1-2), 51-84.
- Sjöberg, E. L. (1978). Kinetics and mechanism of calcite dissolution in aqueous solutions at low temperatures. *Stockholm Contrib. Geol.*, 32, 92 pp.
- Sjöberg, E. L., and Rickard, D. (1983). "The influence of experimental design on the rate of calcite dissolution." *Geochimica et cosmochimica acta*, 47(12), 2281-2285.
- Stocks-Fischer, S., Galinat, J. K., and Bang, S. S. (1999). "Microbiological precipitation of CaCO3." *Soil Biology and Biochemistry*, 31(11), 1563-1571.
- Stumm, W., and Morgan, J. J. (2012). *Aquatic chemistry: chemical equilibria and rates in natural waters*. John Wiley & Sons.
- Parkhurst, D. L., and Appelo, C. A. J. (2013). Description of input and examples for PHREEQC version 3: a computer program for speciation, batch-reaction, one-dimensional transport, and inverse geochemical calculations (No. 6-A43). US Geological Survey.